

# Pressure Control of Hydraulic Servo System Using Proportional Control Valve

Kyong-Uk Yang\*, In-Ho Oh\*\* and Ill-Yeong Lee\*\*\*

(Received August 5, 1998)

The purpose of this study is to develop a control scheme for the hydraulic servo system which can rapidly control the pressure in a hydraulic cylinder with very short stroke. Compared with the negligible stroke of the cylinder in the system, the flow gain of the proportional pressure control valve constituting the hydraulic servo system is relatively large and the time delay on the response of the valve is quite long. Therefore, the pressure control system, in this study tends to get unstable during operations. Considering the above mentioned characteristics of the system, a two-degree-of-freedom control scheme, composed of the I-PDD<sup>2</sup> ... feedback compensator and the feedforward controller, is proposed. The reference model scheme is used in deciding the parameters of the controllers. The validity of the proposed control scheme is confirmed through the experiments.

**Key Words :** Pressure Control, Two-Degree of Freedom Control, Proportional Pressure Control Valve

## 1. Introduction

The hydraulic pressure control systems are widely used in various industrial fields; the hydraulic system for clutch actuation in the automatic transmission of a vehicle, the anti-lock brake system of a vehicle, the hydraulic injection molding machine and so forth.

The electro-hydraulic servo valve or the proportional control valve is usually used as an actuator and the open loop or the closed loop control method can be adopted as the control scheme. The open loop control system might be used in the systems in which the accuracy and the fast response are not required. The open loop pressure control systems need control valves having an internal pressure feedback mechanism (UCHIDA Co., 1990). On the other hand, the closed loop control system is preferred in the systems require the higher level of accuracy and the fast response. The digital control equipments

make it possible to apply the highly efficient control algorithm to the closed loop control system.

The purpose of this study is to develop a control scheme that can accurately control the hydraulic pressure control system consisting of a proportional pressure control valve and a hydraulic cylinder with nearly 'zero' stroke (Yang et al., 1995), which can be found in the clutch actuator in the automatic transmission of a vehicle. While the stroke of the cylinder is nearly 'zero', the flow gain of the control valve is very large and the time delay appearing on the response of the valve is quite large (UCHIDA Co., 1990). Therefore, the system we are interested in tends to become unstable with ease. The control algorithm should be carefully chosen so that it can easily be applied to the practical use.

Taking into account the characteristics of the system and the limitations on choosing the control algorithm, a two-degree-of-freedom control scheme is designed. The control scheme is composed of an I-PDD<sup>2</sup> ... feedback compensator and a feedforward controller (Kitamori, 1979). The parameters of controller are chosen by means

---

\* Yosu National University, Yosu, Korea

\*\* Korea Maritime University, Pusan, Korea

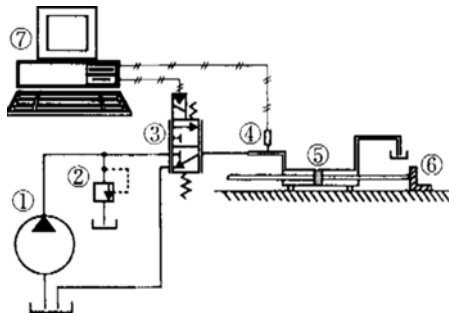
\*\*\* Pukyong National University, Pusan, Korea

of the reference model approach (Sigemasa et al., 1983; Tanaka and Ashikaga, 1992). The validity of the control scheme is confirmed through experiments.

## 2. Modelling of the System

### 2.1 Description of the system

The hydraulic pressure control system in this study is illustrated in Fig. 1. One of two ports is vented to the atmosphere so that the cylinder acts as a single acting cylinder. And the piston rod is blocked by the stopper ⑥ in order that the stroke of the cylinder becomes nearly zero just as in the clutch actuator in the automatic transmission of a vehicle. The pipe connecting the cylinder and the valve is short and burly. The cracking pressure of the relief valve is set at 2.0MPa.



- ① hydraulic pump ② relief valve  
 ③ proportional pressure control valve  
 ④ pressure transducer ⑤ hydraulic cylinder(volume)  
 ⑥ stopper ⑦ computer

Fig. 1 Configuration of the pressure control system.

The pressure transducer ④ senses the pressure value in the cylinder and sends the signal to the personal computer used as a controller and data recorder by way of a Analog-Digital convertor. And the control signal calculated in the controller is sent to the control valve through a Digital-Analog convertor. Table 1 describes the specifications of the equipments and instruments of the experimental apparatus.

As the stroke of the cylinder is nearly zero, the flow rate into the cylinder can be obtained as follows:

$$\frac{\Delta V_c}{\Delta t} = \frac{V_c \Delta P_t}{\beta_o} \cdot \frac{1}{\Delta t} \quad (1)$$

where  $V_c$  is the volume of cylinder,  $\Delta P_t$  is the variation of pressure in the cylinder,  $\beta_o$  is the bulk modulus of oil.

If  $V_c$ ,  $\Delta P_t$ ,  $\beta_o$  and  $\Delta t$  are of 105 cm<sup>3</sup>, 1 MPa,  $1.6 \times 10^9$  N/m<sup>2</sup> and 0.1 s respectively, then the flow rate will be  $3.9 \times 10^{-4}$  l/min. It is hard to find the pressure control valve of which the nominal flow rate is as small as  $3.9 \times 10^{-4}$  l/min.

The smallest pressure control valve of which the nominal flow rate at the pressure difference of 2.0 MPa is 9.5 l/min was chosen for the experiment. But the flow rate of the valve is still much larger than that of the required in the system. It means the flow gain of the valve is very large and the pressure in the cylinder might change too fast and fluctuate when the valve spool moves from the neutral position. It may deteriorate the stability of the system. Moreover, quite a long time

Table 1 Specification of instruments used in the experiment.

instruments	specification	manufacturer	model number model number
hydraulic cylinder	5.0 MPa, Max	TAIYO	35H-2D Hydraulic CYL.
hydraulic pump	12.2 cm <sup>3</sup> /rev	Yuken	F-PV2R1-12-R
pressure sensor	0~10 MPa	Sensotec	9E02-P3-100
A/D converter	resolution 12 bit A/D : 16, D/A : 2	Adventech	PCL-812
PCV	15 l/min, 4.9 MPa	Uchida	3DREP6
PC intel 386	CPU 33 MHz	Samsung	SPC

delay on the response of the valve might deteriorate the quality of control.

The above mentioned characteristics and conditions of the system should be seriously considered in choosing the experimental equipments and designing the control system.

**2.2 Modelling**

Fig. 2 shows the schematic of the 3-way proportional pressure control valve and the cylinder used in this study. When the valve spool moves from the neutral position, the flow rate through the throttle opening in the valve which connects the pump outlet and the cylinder  $Q_l$  and the flow rate through the other throttle opening connecting the cylinder and the reservoir  $Q_r$  can be represented as in Eqs. (2) and (3). And the flow rate through the oil passage into the internal feedback mechanism in the valve  $Q_f$  can be described as Eq. (4).

$$Q_l = C_{d1} w (u_s + x_s) \sqrt{\frac{2}{\rho} (P_s - P_l)} \quad (2)$$

$$Q_r = C_{d2} w (u_s - x_s) \sqrt{\frac{2}{\rho} P_l} \quad (3)$$

$$Q_f = -A_s \frac{dx_s}{dt} \quad (4)$$

where  $C_{d1}$  and  $C_{d2}$  indicates the discharge coefficients of the throttle openings in the valve,  $A_s$  is the sectional area of the spool,  $w (= \pi \cdot d_s, d_s$  is the diameter of spool section) is the area gradient of the throttle openings,  $u_s$  is the overlap of spool,  $x_s$  is the displacement of spool,  $P_s$  is the supply pressure and  $P_l$  is the load pressure in the

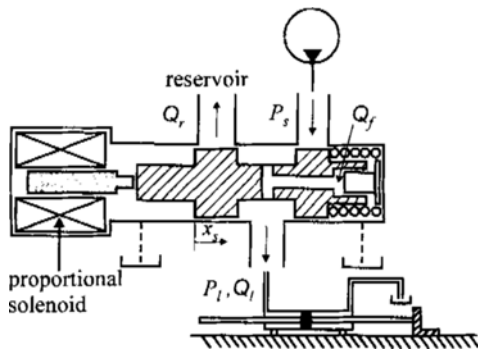


Fig. 2 Schematic diagram of the proportional pressure control valve.

cylinder.

The nonlinear equations, Eqs. (2) and (3), can be linearized as follows.:

$$\Delta Q_l = \frac{\partial Q_l}{\partial x_s} \Delta x_s + \frac{\partial Q_l}{\partial P_l} \Delta P_l \quad (5)$$

$$\Delta Q_r = \frac{\partial Q_r}{\partial x_s} \Delta x_s + \frac{\partial Q_r}{\partial P_l} \Delta P_l \quad (6)$$

As the displacement of the cylinder is nearly zero, the application of the continuity makes the load flow rate  $Q_l$  equal to the following.

$$Q_l = Q_f + \frac{V}{\beta_e} \frac{dP_l}{dt} \quad (7)$$

where  $V$  is the volume of the cylinder and the pipe and  $\beta_e$  indicates the equivalent bulk modulus of oil.

The relation between the solenoid force  $F_s$  and the input current  $i$  can be described as Eq. (8) considering the dynamic characteristic of the proportional solenoid (Lu, 1981). The relation between the spool displacement and the solenoid force acting on the spool is described in Eq. (9) where the term indicating the inertia force is ignored.

$$K_i i = C_1 \frac{dF_s}{dt} + C_2 F_s \quad (8)$$

$$F_s = C_3 \frac{dx_s}{dt} + C_4 x_s + A_s P_l \quad (9)$$

where  $K_i$  is the gain of solenoid and  $C_1, C_2, C_3$  and  $C_4$  are constants.

The Laplace transforms of the Eqs. (5) ~ (9) can be as follows:

$$Q_l(s) = K_1 X_s(s) + K_2 P_l(s) \quad (5')$$

$$Q_r(s) = K_3 X_s(s) + K_4 P_l(s) \quad (6')$$

$$Q_l(s) = -A_s s X_s(s) + \frac{V}{\beta_e} s P_l(s) \quad (7')$$

$$K_i I(s) = C_1 s F_s(s) + C_2 F_s(s) \quad (8')$$

$$F_s(s) = C_3 s X_s(s) + C_4 X_s(s) + A_s P_l(s) \quad (9')$$

where,  $K_1, K_2, K_3$  and  $K_4$  are the partial derivations, of  $\partial Q_l / \partial x_s, \partial Q_l / \partial P_l, \partial Q_r / \partial x_s$  and  $\partial Q_r / \partial P_l$ , respectively, at the neutral position of the operating range.

The transfer function between  $P_l(s)$  and  $I(s)$  can be obtained from the Laplace transforms as follows:

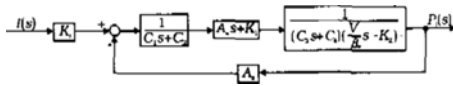


Fig. 3 Block diagram of the object pressure control system.

$$\frac{P_f(s)}{I(s)} = \frac{K_i(K_1 + A_s s)}{(C_1 s + C_2) \left\{ (C_3 s + C_4) \left( \frac{V}{\beta_e} s - K_2 \right) + A_s (K_1 + A_s s) \right\}} \quad (10)$$

The block diagram of the system is shown in Fig. 3.

### 3. Design of Two-Degree of Freedom Control System with FF-I-PDD<sup>2</sup>... Controller

The pressure control system in this study has a few shortcomings as mentioned in Sec. 2.2. Therefore, the gain of forward path controller can not be increased without affecting the system stability, and the good control quality is difficult to achieve due to the long time delay of the valve. Moreover, the computation time of the control algorithm should be short enough for an easy application to the industrial use.

The authors chose the two-degrees of freedom control scheme based on the I-PDD<sup>2</sup>... feedback compensator with feedforward controller (Kitamori, 1979). Because the feedforward controller is not included in the feedback closed loop, the feedforward controller is able to offset the zeros by the poles or to shift the poles of the system without affecting the roots of the characteristic equation of one-degree of freedom control system (Kuo, 1991).

Figure 4 represents FF-I-PDD<sup>2</sup>... control system where  $y(t)$  is the control output,  $e(t)$  is the error and  $u(t)$  is the control signal.

The reference input  $r(t)$  and the disturbance  $d(t)$  are expressed as the polynomials of time  $t$ .

$$r(t) = \sum_{j=0}^n r_j t^j \quad (11)$$

$$d(t) = \sum_{j=0}^n d_j t^j \quad (12)$$

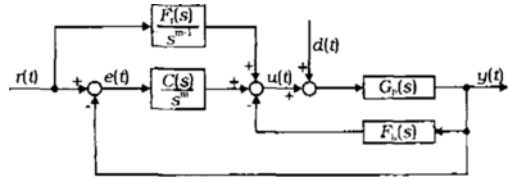


Fig. 4 Block diagram of FF-I-PDD<sup>2</sup>... control system.

The plant  $G_p(s)$ , the forward path controller  $C(s)/s^m$ , the feedback compensator  $F_b(s)$  and the feedforward controller  $F_f(s)/s^{m-1}$  are described as the polynomials of Laplace operator  $s$ .

$$G_p(s) = \frac{1}{G(s)} = \frac{1}{g_0 + g_1 s + g_2 s^2 + \dots + g_n s^n} \quad (13)$$

$$C(s) = C_0 + C_1 s + C_2 s^2 + \dots + C_n s^n \quad (14)$$

$$F_b(s) = F_{b0} + F_{b1} s + F_{b2} s^2 + \dots + F_{bn} s^n \quad (15)$$

$$F_f(s) = F_{f0} + F_{f1} s + F_{f2} s^2 + \dots + F_{fn} s^n \quad (16)$$

where the order of integrator  $m$  and the order of numerator in the forward path controller are determined by the type of plant (Kim, 1991). And the order of feedback compensator represented in Eq. (11) is determined by the order of plant (Kitamori, 1979).

The coefficients of the forward path controller, feedback compensator and feedforward controller should be optimized to make the controller efficient. In this study, the reference model method suggested by Kitamori (1973) is used in determining the parameters of FF-I-PDD<sup>2</sup> controller.

The reference model should be designed to satisfy the following conditions.

First, the steady state error  $e(t)$  must be zero.

$$\lim_{t \rightarrow \infty} e(t) = \lim_{n \rightarrow \infty} s e(s) = 0 \quad (17)$$

Second, the real part of all the roots of polynomial representing the characteristic equation of the close loop control system must be negative.

Third, the response characteristic of the system suits the conditions required.

The reference model  $M_r(s)$  relating the control output  $y(s)$  to the reference input  $r(s)$  is sup-

posed to be as follows:

$$M_r(s) = \frac{\beta_0 + \beta_1 \alpha_1 \sigma s + \beta_2 \alpha_2 (\sigma s)^2 + \dots + \beta^{n_\beta} \alpha^{n_\beta} (\sigma s)^{n_\beta}}{1 + \alpha_1 \sigma s + \alpha_2 (\sigma s)^2 + \dots + \alpha^{n_\alpha} (\sigma s)^{n_\alpha}} \quad (18)$$

$$y(s) = M_r(s) \cdot r(s) \quad (19)$$

where the order of denominator polynomial  $n_\alpha$  is larger than the order of numerator polynomial  $n_\beta$  and  $\sigma$  is the conversion factor of rise time.

The error  $e(s)$  between the reference input  $r(s)$  and the control output  $y(s)$  can be represented as Eq. (20)

$$e(s) = r(s) - y(s) \quad (20)$$

Therefore, the error becomes as follows:

$$e(s) = (1 - \beta_0) + \alpha_1 (1 + \beta_1 (\sigma s)) + \dots + \alpha^{n_\alpha} (1 - \beta^{n_\beta}) (\sigma s)^{n_\beta} + \alpha^{n_{\beta+1}} (\sigma s)^{n_{\beta+1}} + \dots + \alpha^{n_\alpha} (\sigma s)^{n_\alpha} / 1 + \alpha_1 \sigma s + \alpha_2 (\sigma s)^2 + \dots + \alpha^{n_\alpha} (\sigma s)^{n_\alpha} \quad (21)$$

The Laplace transform of Eq. (11) can be described as

$$r(s) = \sum_{j=0}^n \frac{r_j}{s^{j+1}} \quad (22)$$

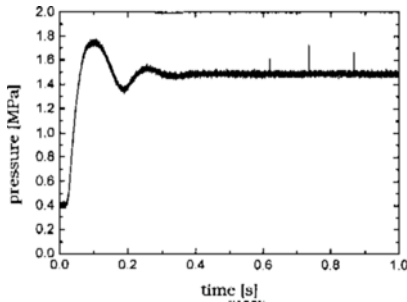
When Eq. (17) is substituted to Eqs. (21) and (22), the followings are obtained.

$$\beta_i = 1 \quad (i = 0, 1, 2, \dots, n) \quad (23)$$

$$n < n_\beta \quad (24)$$

Consequently, the reference model  $M_r(s)$  can be described as Eq. (25).

$$M_r(s) = 1 + \alpha_1 \sigma s + \alpha_2 (\sigma s)^2 + \dots + \alpha^{n_\alpha} (\sigma s)^{n_\alpha} + \beta_{n+1} \alpha_{n+1} (\sigma s)^{n+1} + \dots + \beta^{n_\beta} \alpha^{n_\beta} (\sigma s)^{n_\beta} / 1 + \alpha_1 \sigma s + \alpha_2 (\sigma s)^2 + \dots + \alpha^{n_\alpha} (\sigma s)^{n_\alpha} \quad (25)$$



(b) variation of target pressure:  $0.4 \geq 1.5$  MPa

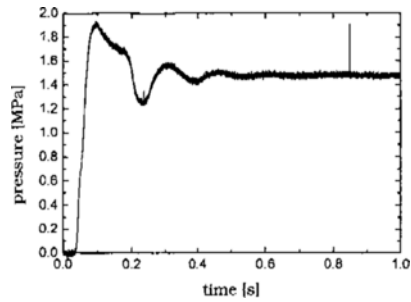
The controller can be designed by coinciding all the terms of the transfer function indicating the closed loop control system with the corresponding terms of the reference model.

## 4. Identification of the System and Design of the Control System

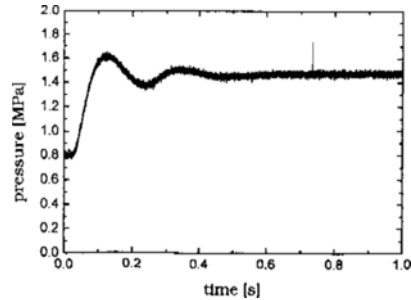
### 4.1 Identification of the system

The constants  $K_1$  indicating the flow gain of the valve and  $K_2$  indicating the flow-pressure coefficient of the valve in Eq. (10) vary when the load pressure  $P_l$  and the flow rate  $Q_l$  go farther from the value when the valve spool is at the neutral position in operating range. There exist difficulties in inspecting the dynamic characteristic of solenoid and measuring the parameters of valve. Therefore, the transfer function of the system was derived from the experimental step response of the system.

Figure 5 shows the step response of the system resulting from the experiment. (a), (b) and (c) are the results when the input signals are stepped up from 0 MPa to 1.5 MPa, 0.4 MPa to 1.5 MPa



(a) variation of target pressure:  $0 \geq 1.5$  MPa



(c) variation of target pressure:  $0.8 \geq 1.5$  MPa

Fig. 5 Experimental results of step response of the pressure control system under open loop control.

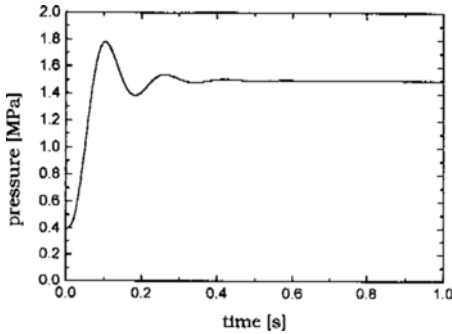


**Fig. 6** Simulation result of step response of the pressure control system under open loop control (variation of target pressure:0.4 → 1.5 MPa).

and 0.8 MPa to 1. 5 MPa, respectively. The settling times in (a), (b) and (c) are 500ms, 300ms and 430ms and the time delays are 37ms, 25ms and 30ms, respectively.

In the response curve appearing in (a), non-linearity exists and the time delay is longer than those in (b) and (c). It seems that the large overlap and the large static friction due to no dither effect causes these deficiency. The response with quite a good linearity shown in (b) was chosen for the identification of the system(Jung, Lee and Yang, 1993). The transfer function was identified as a third order system and described as follows:

$$G_p(s) = \frac{1}{0.000012897s^3 + 0.0008977s^2 + 0.03586s + 1} \tag{26}$$

The computed result of the step response of the system represented by Eq. (26) is shown in Fig. 6.

**4.2 Design of FF-I-PDD<sup>2</sup>... controller**

**4.2.1 FF-I-PD controller for the step input**

When the reference input signal is a step signal, the order of integrator in the forward path controller becomes the first and the feedback compensator might be a PD compensator because the type of the system is zero(Kim, 1991) and the system is of the third order. Therefore, the controller becomes the FF-I-PD controller shown in Fig. 7.

The loop transfer function becomes the fourth

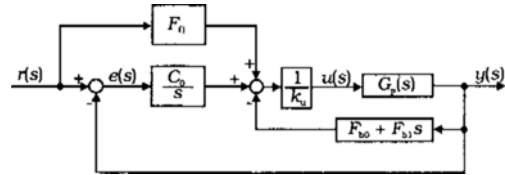


**Fig. 7** Block diagram of FF-I-PD control system when stepwise input signal applied.

order and the transfer function indicating the whole system  $G_{PL}(s)$  can be described as

$$G_{PL}(s) = \frac{y(s)}{r(s)} = \frac{F_{f1}s + C_0}{g_3s^4 + g_2s^3 + (F_{b1} + g_1)s^2 + (F_{b0} + g_0)s + C_0} \tag{27}$$

where  $g_0 = 1/k_u$ ,  $g_1 = 2\zeta/\omega_n k_u$ ,  $g_2 = 2\zeta/\omega_n^2 k_u$  and  $g_3 = 1/\omega_n^2 k_u$ .  $k_u$  is the controller gain,  $\zeta$  is the damping coefficient of the system and  $\omega_n$  is the natural frequency of the system.

The reference model required in this case can be derived from Eq. (25) as follows:

$$G_m(s) = \frac{C_0(1 + \alpha\beta\sigma s)}{C_0(1 + a_1\sigma s + a_2r^2s^2 + a_3\sigma^3s^3 + a_4\sigma^4s^4)} \tag{28}$$

The coefficients of denominator polynomial  $a_1$ ,  $a_2$ ,  $a_3$  and  $a_4$  can be represented as  $a_i = (1 - \alpha) \cdot b_i + \alpha \cdot c_i$  where  $\alpha$  is the weighting factor,  $b_i$  is the coefficient of denominator polynomial composed of negative real roots and  $c_i$  is the coefficient of denominator polynomial composed of negative complex roots(Shigemasa et al., 1983; Tanaka, 1992). The coefficients are determined so that the response characteristic of the reference model satisfies what is desired.

Figure 8 shows the computed step responses of the 4th order reference models when  $\beta$  is set at 0 and  $\alpha$  is varied from 0 to 1.0 by the increment of 0.2. On the other hand, when  $\alpha$  is fixed at 0 and  $\beta$  is varied from 0 to 1.0, the step responses are shown in Fig. 9. Figures 8 and 9 clearly indicate that the change of  $\alpha$  affects the change of settling time and the value of  $\beta$  influences the rise time on the step responses. The root loci of characteristic equation of the reference model according to the change of weighting factor  $\alpha$  were shown in Fig. 10. As the value of  $\alpha$

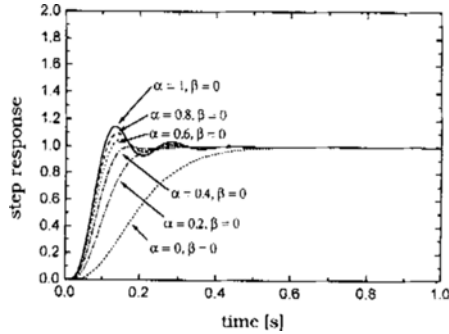


Fig. 8 Simulated step responses of reference model with various  $\alpha$ -parameter values.

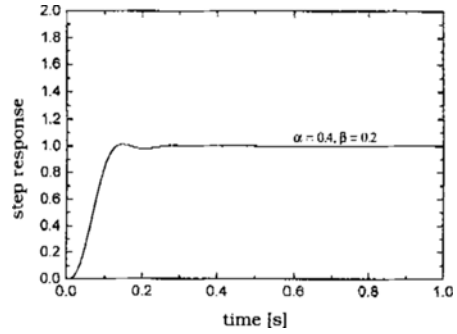


Fig. 11 Simulated step response of the objective reference model ( $\alpha=0.4, \beta=0.2$ ).

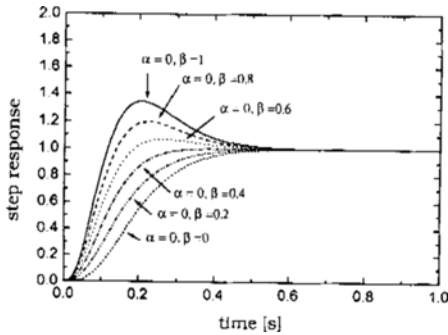


Fig. 9 Simulated step responses of reference model with various  $\beta$ -parameter values.

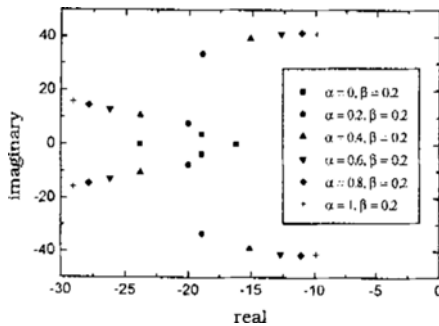


Fig. 10 Pole allocation of reference models.

increases, the root loci approach to the imaginary axis.

The fact that the system is more stable as the value of  $\alpha$  and  $\beta$  are smaller and the sensitivity of the system improves as the value of  $\alpha$  and  $\beta$  is getting larger can be known from Figs. 8~10. Therefore, the value of  $\alpha$  and  $\beta$  are determined based on a proper trade off considering the system characteristic (Tanaka, 1992).

In this study, the reference model was designed

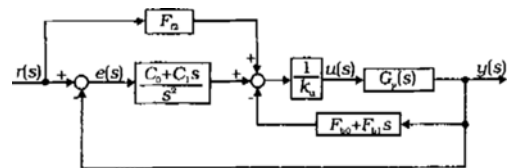


Fig. 12 Block diagram of FF-I<sup>2</sup>-PD control system when ramp input signal applied.

by setting  $\alpha=0.4$  and  $\beta=0.2$ . The parameters of FF-I-PD controller obtained from substituting Eq. (27) to Eq. (28) are as follows:

$$C_0=12.4942, F_{f1}=0.21812, F_{b0}=0.9058, F_{b1}=0.00335$$

And the computed step response of the designed control system is shown in Fig. 11.

#### 4.2.2 FF-I<sup>2</sup>-PD controller for the ramp input

When the ramp signal is applied as the reference input, the order of integrator should be the second in order to eliminate the steady state error. So, the loop transfer function becomes the fifth order. The FF-I<sup>2</sup>-PD controller is shown in Fig. 12.

The transfer function of the system  $G_{PL}(s)$  can be represented as follows:

$$G_{PL}(s) = \frac{y(s)}{r(s)} = \frac{F_f 2s^2 + C_1 s + C_0}{g_3 s^5 + g_2 s^4 + (f_{b1} + g_1) s^3 + (f_{b0} + g_0) s^2 + C_1 s + C_0} \quad (29)$$

The reference model

$$G_m(s) =$$

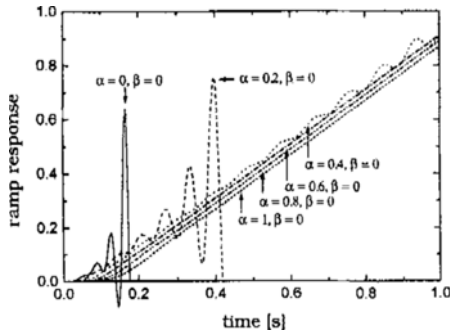


Fig. 13 Simulated ramp responses of reference model with various  $\alpha$ -parameter values.

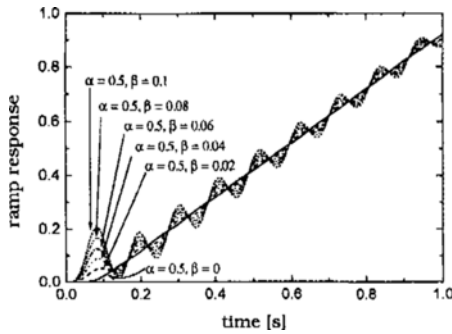


Fig. 14 Simulated ramp responses of reference model with various  $\beta$ -parameter values.

$$\frac{(C_0 + C_1s)(1 + a\beta\sigma^2s^2)}{(C_0 + C_2s)(1 + a_1\sigma s + a_2\sigma^2s^2 + a_3\sigma^3s^3 + a_4\sigma^4s^4 + a_5\sigma^5s^5)} \quad (30)$$

As in the case of the step input, the parameters of reference model  $\alpha$  and  $\beta$  are determined by carefully inspecting the computed responses shown in Figs. 13 and 14. And the reference model is designed by trade off.

Figure 13 shows the computed ramp responses of reference models when  $\beta$  is fixed at 0 and  $\alpha$  is varied from 0 to 1.0. The computed responses of reference models when  $\beta$  is varied from 0 to 0.1 by the increment of 0.02 with  $\alpha$  remaining fixed at 0.5 are shown in Fig. 14. They indicate that the response curves are more sensitive to  $\alpha$  and  $\beta$ . It seems that these phenomenon were caused by the fact that the time delay on the response of the valve is quite long and the flow gain of the valve is very large. Therefore, there is a limit on improving the sensitivity of the controller.

The parameters of the reference model  $\alpha$  and  $\beta$  are determined as  $\alpha=0.5$  and  $\beta=0.01$ . And the

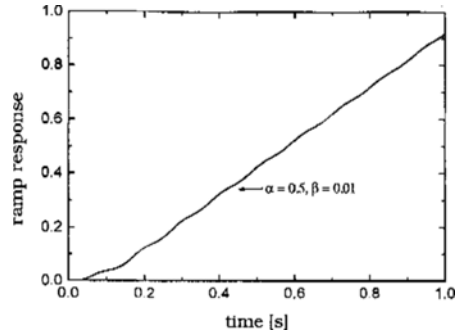


Fig. 15 Simulated ramp response of the objective reference model ( $\alpha=0.5, \beta=0.01$ ).

controller parameters are obtained from the reference model as follows:

$$C_0=231.4364, C_1=20.02, F_{f1}=0.0007, F_{b0}=0.19, F_{b1}=0.00169$$

The computed ramp response of the FF-I<sup>2</sup>-PD control system is shown in Fig. 15.

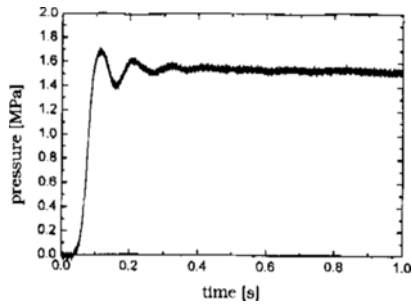
### 5. Experimental Results and Discussions

The experiments on the closed loop pressure control system were carried out to investigate the effects of the controller on the response characteristics of the system. The sampling interval was set to be 5ms during the experiments.

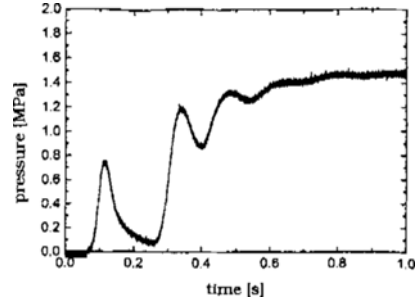
Figure 16 shows the experimental step responses on the FF-I-PD control system designed in accordance with the process mentioned in Sec. 4.2.1. The (a), (b) and (c) are the results when the reference inputs were stepped up from 0 MPa to 1.5 MPa, 0.4 MPa to 1.5 MPa and 0.8 MPa to 1.5 MPa, respectively. The appearance of the overshoots on the response curves in (a) and (c) compared with that in (b) seems to be caused by the fact that the system model used in designing the FF-I-PD controller is identified from the result shown in Fig. 5(b). The time delay appearing in (a) is longer than those in (b) and (c). And this phenomena is the same as in Fig. 5.

The settling time on the response curve shown in Fig. 16(b) is about 100ms and it fairly coincides with that in Fig. 11, the computed result.

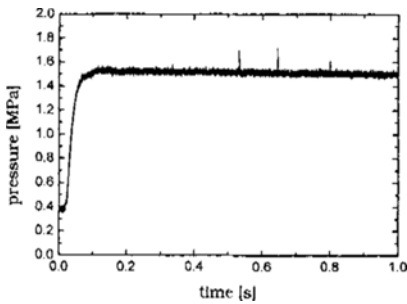




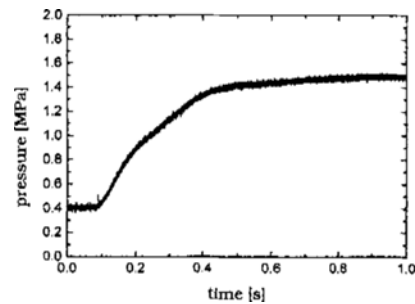
(a) variation of target pressure:  $0 \geq 1.5$  MPa



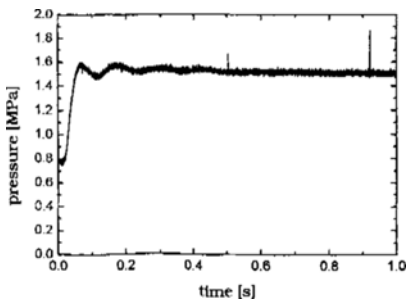
(a) variation of target pressure:  $0 \geq 1.5$  MPa



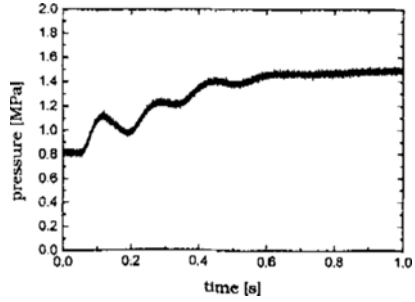
(b) variation of target pressure:  $0.4 \geq 1.5$  MPa



(b) variation of target pressure:  $0.4 \geq 1.5$  MPa



(c) variation of target pressure:  $0.8 \geq 1.5$  MPa



(c) variation of target pressure:  $0.8 \geq 1.5$  MPa

**Fig. 16** Experimental results of step response of the pressure control system under closed loop control with FF-1-PD controller.

**Fig. 17** Experimental results of ramp response of the pressure control system under closed loop control with FF-1<sup>2</sup>-PD controller.

The rise time in Fig. 16(b) is shorter than that in Fig. 11 and it seems to be caused by the influence of the discrepancy between the real system and the identified model.

The time delay in Fig. 16(b) is 20ms and it is a little shorter than that appearing in Fig. 5(b), the experimental step response on the open loop system. The improvement of control quality by the FF-1-PD control is known from the comparison of the response curve shown in Fig. 16(b) with that shown in Fig. 5(b).

Figure 17 shows the ramp responses resulting

from the experiments on the FF-1<sup>2</sup>-PD control system mentioned in Sec. 4.2.2. (a), (b) and (c) are the results when the reference inputs were increased from 0 MPa to 1.5 MPa, 0.4 MPa to 1.5 MPa and 0.8 MPa to 1.5 MPa, respectively. The response curve shown in (b) is fairly good compared with those in (a) and (c), which show the pressure fluctuations. It might be due to the fact that the flow gain of the valve is very large in addition to that the system model is identified from the result shown in Fig. 5(b).

There are some limits in improving the ramp

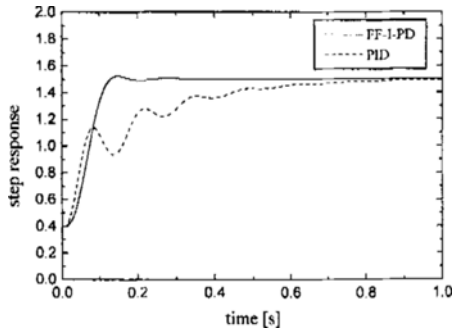


**Fig. 18** Simulation results of step response of the pressure control system under FF-I-PD and PID controller.

response but the careful design of the controller based on the adequately identified system model can make it possible to improve the control quality.

The widely used PID controller was designed by Ziegler-Nichols method (JSME, 1993). And the response characteristics of the PID control system resulting from computations were compared with those of the FF-I-PD control system and the FF-I<sup>2</sup>-PD control system for the purpose of obtaining the objective data on the validity of the two-degree of freedom control scheme.

Figure 18 shows the computed step responses of the PID control system and FF-I-PD control system. It indicates that the response characteristic of the PID control system is inferior to that of the FF-I-PD control system.

The computed ramp responses of those two control systems are shown in Fig. 19. It also indicates that the two-degrees of freedom control system is superior to the PID control system. There is a steady state error on the response curve of PID control system because the lack of integrator make the system do not follow up the ramp reference input.

The two-degrees of freedom control scheme based on FF-I-PDD<sup>2</sup>... controller can improve not only the system stability but also the system sensitivity by decreasing the influences of disturbance and noise.

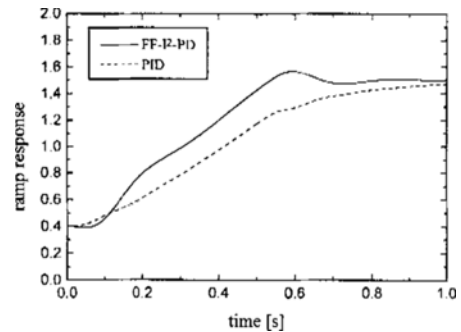


**Fig. 19** Simulation results of ramp response of the pressure control system under FF-I<sup>2</sup>-PD and PID controller.

## 6. Conclusion

The two-degrees of freedom control scheme was established in this study in order to efficiently control the hydraulic pressure control system, consists of a proportional pressure control valve and a cylinder of which the stroke is nearly zero. The validity of the control scheme established was confirmed through the experiments.

The results obtained in this study are briefed as follows.

(1) The application of the closed loop control method to the hydraulic pressure control system effectively shortens the time delay which appears on the response of the valve.

(2) The FF-I-PDD<sup>2</sup>... controller enabled the system to improve the stability and sensitivity of the system even with the low gain of forward path controller.

(3) The reference model method made it convenient to determine the controller parameters in designing the control system.

(4) The careful design of controller by means of the adequately identified system model in operating range can help improve the control quality even though there are some limits in improving the ramp response of the system.

## Reference

Japan Society of Mechanical Engineers, 1993, *Mechatronics and Control Engineering*, Japan, pp. 142-147.

- Jung, Y. G., Lee, I. Y. and Yang, J. H., 1993, "Constant Speed Control of Shaft Generating System Driven by Hydrostatic Transmission for Ship Use," *Transactions of the Korean Society of Mechanical Engineers*, Vol. 17, No. 8, pp. 1999~2010.
- Kim, J. S., 1991, *Linear Control of Dynamic Systems*, Cheong-Moon-Gak, Seoul in Korea, pp. 119~122.
- Kitamori, T., "A Method of Control System Design Based upon Partial Knowledge about Controlled Processes," *Transactions of the Society of Instrument and Control Engineers*, Japan, Vol. 15, No. 3, pp. 135~141.
- Kuo, B. C., 1991, *Automatic Control System*, Sixth Edition, Prentice-Hall Inc., pp. 325~425.
- Lu, Y., 1981, *Entwicklung Vorgesteuerter Proportionalventil mit 2-Wege-Einbauventil als Stellglied und mit Geräteinterne Rückführung*, Ph. D. Thesis, T. H. Aachen.
- Shigemasa, T., Takaki, Y., Ichikawa, Y. and Kitamori, T., 1983, "A Practical Reference Model for Control System Design," *Transactions of the Society of Instrument and Control Engineers*, Japan, Vol. 19, No. 7, pp. 592~594.
- Tanaka, Y. and Ashikaga, M., 1992, "A Low-Sensitive Robust Control for a Gas Turbine," *Transactions of the Society of Instrument and Control Engineers*, Japan, Vol. 28, No. 2, pp. 255~263.
- Tanaka, Y., 1992, " $\alpha$  Parameter for Robust Control Design," *Transactions of the Society of Instrument and Control Engineers*, Japan, Vol. 28, No. 12, pp. 1501~1503.
- UCHIDA Oil Hydraulic MFG Co., 1990, Total Catalog, Japan, pp. 564~589.
- Yang, K. U., Yun, S. N., Lee, I. Y., Lee, D. G. and Huh, P. Y., 1995, "Dynamic Characteristics Improvement of Semi-Automatic Transmission Driven by Hydraulic Power for Construction Vehicles", *Proceedings of The 2nd International Symposium on Fluid Power transmission and Control*, Shanghai, China, pp. 155~160.